Optical characterization of ZnO nanopillars on Si and macroporous periodic Si structure

M. V. Castro Meira, A. Ferreira da Silva, G. Baldissera, C. Persson, J. A. Freitas, N. Gutman, A. Saar, Omer Nur and Magnus Willander

Linköping University Post Print

N.B.: When citing this work, cite the original article.

Optical characterization of ZnO nanopillars on Si and macroporous periodic Si structure

M. V. Castro Meira, A. Ferreira da Silva, G. Baldissera, C. Persson, J. A. Freitas et al.

Related Articles

Radiative damping suppressing and refractive index sensing with elliptical split nanorings
Appl. Phys. Lett. 100, 203119 (2012)

Symmetrically tunable optical properties of InGaN/GaN multiple quantum disks by an external stress
Appl. Phys. Lett. 100, 171916 (2012)

Interference effects on indium tin oxide enhanced Raman scattering
J. Appl. Phys. 111, 033110 (2012)

Optical properties of a-plane (Al, Ga)N/GaN multiple quantum wells grown on strain engineered $Zn_{1-x}Mg_xO$ layers by molecular beam epitaxy
Appl. Phys. Lett. 99, 261910 (2011)

Spectrally and temporarily resolved luminescence study of short-range order in nanostructured amorphous ZrO_2

J. Appl. Phys. 110, 103521 (2011)

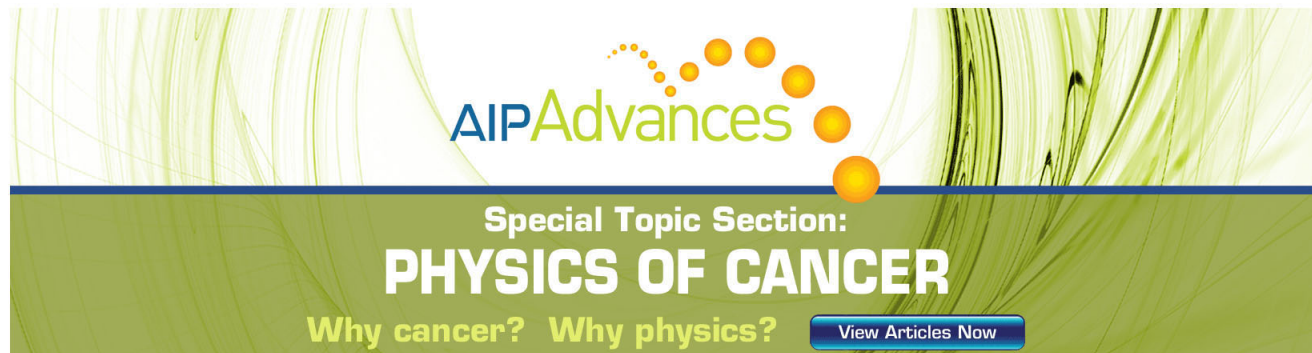## Additional information on J. Appl. Phys.

Journal Homepage: http://jap.aip.org/
Journal Information: http://jap.aip.org/about/about_the_journal
Top downloads: http://jap.aip.org/features/most_downloaded
Information for Authors: http://jap.aip.org/authors

Optical characterization of ZnO nanopillars on Si and macroporous periodic Si structure

M. V. Castro Meira,[1,2] A. Ferreira da Silva,[2] G. Baldissera,[3] C. Persson,[3,4] J. A. Freitas Jr.,[5] N. Gutman,[6] A. Sa'ar,[6] O. Nur,[7] and M. Willander[7,a)]

[1]CETEC-Universidade Federal do Recôncavo da Bahia, Cruz das Almas-Ba 44380-000, Brazil
[2]Instituto de Física, Universidade Federal da Bahia, Ondina, Salvador-Ba 40210-340, Brazil
[3]Department of Materials Science and Engineering, Royal Institute of Technology, SE-100 44 Stockholm, Sweden
[4]Department of Physics, University of Oslo, P.O. Box 1048 Blindern, NO-0316 Oslo, Norway
[5]Naval Research Laboratory, ESTD, Washington, DC 20375-5347, USA
[6]Racah Institute of Physics and the Center for Nanoscience and Nanotechnology, the Hebrew University of Jerusalem, Jerusalem 91904, Israel
[7]Department of Science and Technology, Linköping University, SE-601 74 Norrköping, Sweden

ZnO nanopillars were successfully grown using both the vapor-liquid-solid and the aqueous chemical growth methods on different substrates, such as quartz, n-, and p-type non-porous Si wafer (flat) and microporous periodic Si structure (MPSiS). Scanning electron microscopy was employed to compare sample morphologies. The absorption was calculated employing the GW_0 method, based on the local density approximation, and with the projector augmented wave approach. Experiment and theory show a reasonable agreement when the shape of the optical absorption is considered. The measured absorption of ZnO nanopillars, on different substrates, is lower than that observed for ZnO films on quartz substrate, in the energy gap spectral range. A strong effect of MPSiS substrates on ZnO nanopillar properties is observed. The photoluminescence technique was also employed as an optical characterization. © 2012 American Institute of Physics. [http://dx.doi.org/10.1063/1.4729260]

I. INTRODUCTION

Zinc oxide (ZnO) is a prominent material with large applicability in several fields, for instance, optoelectronics, ultraviolet detectors, biosensors, cosmetic, and medicine.[1–4] It presents low toxicity and good chemical stability. This great versatility of applications is possible mainly because preparation conditions enhance different properties, such as insulator, conductor, semiconductor, photo-electrochemical, luminescent, and piezoelectric. Due to the self organized growth property, ZnO in its nanostructure form can be grown on any substrate. This has enabled the growth of ZnO on a variety of other materials, even on submicrometer glass capillaries.[4] At present many different proto-type devices using ZnO nanostructures have been demonstrated. Currently, research on ZnO nanostructures is one of the most active research fields, and a thorough review of recent achievement of ZnO devices for technical and medical applications can be found in Ref. 4. The recent achievements include optical devices as well as sensors for small volume detection designed for physiological media.[4] Nevertheless, there is lack of important information about optical transitions beyond the direct band gap energy (BGE) of ZnO grown on the microporous periodic Si structure. In this work, we have investigated ZnO nanopillars grown on two-dimensional macroporous periodic silicon (PSi) structure substrates of n- and p-type (n-Psi and p-PSi), and non-

porous, flat silicon (Si), n- and p-type Si (n-Si and p-Si).[1–5] The ZnO nanopillars on the Si substrates have a number of applications beyond of those described above. They can provide, for instance, high quality Si based pH sensors[1] and photonic crystals.[6]

In this work, photoacoustic spectroscopy (PAS) has been used to measure the optical absorption[7,8] of the ZnO films. Using the projector augmented wave (PAW) potentials[9–13] within the local density approximation (LDA) theoretical analysis of ZnO was performed by means of the partially self-consistent GW_0 method.[11,14]

The properties of the ZnO films can be enhanced or implemented by the substrate characteristics. In this work, the photoacoustic technique was used to verify the influence of substrates in the absorption spectra of thin films of ZnO, and luminescence techniques were employed to monitor the film properties.

II. CHARACTERIZATION METHODS

A. Sample preparation

Ordered arrays of trenches and holes in silicon substrates can be fabricated by either direct dry etching of masked substrates or by hydrofluoric (HF) acid based silicon electro-chemical etching. The latter technique has the advantage of producing deep and uniform pattern of holes or pores that can be utilized to form two-dimensional (2D) and three-dimensional (3D) photonic crystals in silicon. Hence, we have utilized the fabrication techniques described in Refs. 15 and 16 to fabricate 2D pore arrays on top of p- and

---

a)Author to whom correspondence should be addressed. Electronic mail: magwi@itn.liu.se.
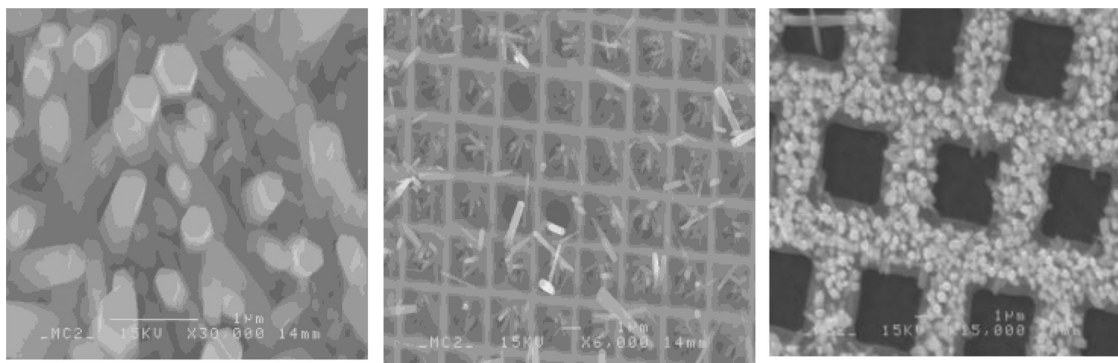
FIG. 1. SEM images are for the p-Si with ZnO optical zoom 30 000× (left); optical zoom 6000× (center); and SEM images are for the n-Si with ZnO optical zoom 15 000× (right).

n-type silicon wafer. In brief, a standard photolithography followed by alkaline anisotropic etching has been used to define 2D pattern of inverted pyramids on top of silicon wafer. Electrochemical etching was performed at room temperature (RT) in the dark for the *p*-type samples and under backside illumination for the *n*-type samples.

ZnO nanopillars were grown on top of the silicon samples using an aqueous chemical growth (ACG) method and a vapor-liquid-solid (VLS) method. There are several different chemical growth methods used to produce ZnO nanostructures. But the most common procedure is that described by Vayssieres *et al.*[17] In this method, zinc nitride $(Zn(NO_3)_26H_2O)$ was mixed with hexamethylenetetramine (HMT $C_6H_{12}N_4$). The substrates were placed in the solution and they were thereafter heated at $90\,°C$ for $180\,min$, upon which rods are formed on the substrate. An equi-molar concentration of HMT and zinc nitride (25 mM) was used.

In the VLS method, the ZnO powder was mixed with carbon powder using a 1:1 weight ratio. The mixture was loaded in a quartz boat and the Si substrate was mounted on top of the powder with a powder-substrate distance of 5 mm. The boat (with the ZnO:C powder and the Si substrate) was placed in the center of the furnace tube. Ar gas flow of 80 sccm was introduced for 5 min to stabilize the environment. The samples were grown for 30 min at $890\,°C$. Fig. 1 shows images of samples by scanning electron microscopy (SEM).

Figure 2 shows the optical microscope images of a ZnO film deposited on a p-Si wafer. Panchromatic image (a) and real color (red/green/blue or RGB) image (b) were acquired using the microscope halogen lamp illumination and a near-UV CCD camera, fitted with a wheel filter, attached to the inverted microscope port. Additional features, related to film inhomogeneities, are easily observed in the optical micrographs ("c" panchromatic and "d" RGB) obtained with the unfocused 325 nm HeCd laser line illumination. Luminescence imaging is a convenient non-destructive approach to visualize morphologies variations and evaluate nanostructured film properties.[18,19]

B. Experimental characterization

PAS has been previously used to determine the optical properties of nanostructured semiconductor materials.[20] The PAS approach consists in illuminating a given material with a modulated light beam and measuring the subsequent tem-

perature fluctuation induced in the sample resulting from the light absorption, due to nonradiative de-excitation processes within the sample. The intermittent heat is transferred into the sealed gas chamber generating an acoustical signal that can be detected by a microphone. The tunable light source of the PAS comprises a high-pressure 1000 W Xenon arc lamp (Osram), modulated to 20 Hz by a chopper (HMS Elektronik, model 220 A) and a scanning monochromator (Sciencentech, model 9010). The spectra were acquired in the spectral region from 350 nm to 700 nm, corresponding to energies from 3.54 eV to 1.77 eV. The light absorbed by the sample, which replaces the cell exit window (the ZnO film side was turned toward the cell cavity), produced a photoacoustic signal, which was detected by a microphone attached to the cell. This microphone was connected to a lock-in amplifier (Stanford Research System, model SR530), which synchronizes the PA signal with the reference pulse from the chopper. Band-pass optical filters were employed to eliminate the contribution from the second order of the diffraction grating, for wavelength smaller than 570 nm.

The sample luminescence was excited at RT with the unfocused 325 nm line of a HeCd laser. Single color optical images, acquired with different magnifications, were obtained with a near-UV CCD described in Sec. II A. The
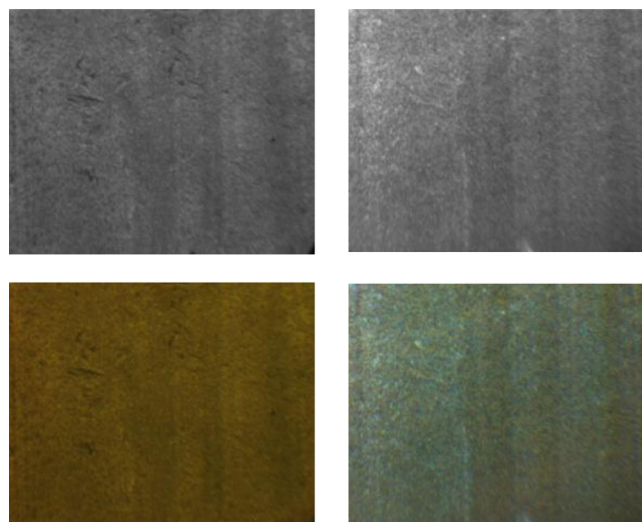

FIG. 2. Optical micrographs of ZnO film on p-Si acquired with the 50× objective lens: superior left laser 325 nm Panchr; superior right Lamp Panchr; inferior left laser 325 nm RGB; inferior right lamp RGB.
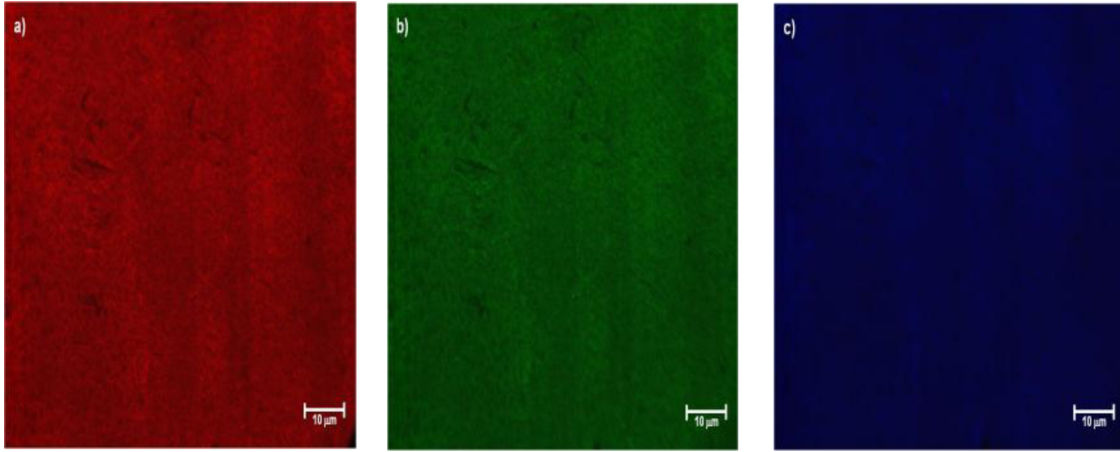
FIG. 3. Single color RGB luminescence images of ZnO film on p-Si captured with 50× objective lens: (a) red, (b) green, and (c) blue.

photoluminescence (PL) spectra were obtained with a fiber optical spectrometer, comprised of an UV extended linear array and a grating blazed at 350 nm, coupled to a near-UV transmitting inverted optical microscope. These techniques were recently applied to rare-earth chloride seeded GaN nanocrystals.[18,19] Both the luminescence images and PL spectra were excited with laser power density of about 10 mW/cm^2.

C. Computational method

Calculations for optical absorption of ZnO were based on the LDA within the density function theory, employing the PAW method.[9–11] The LDA was improved by the partially self-consistent GW$_0$ method where the energies were re-evaluated in the Green's functions[11] In this approach, the method uses quasiparticle energy $E_{n\mathbf{k}}^{QP}$ to correct the energy of the states, using the equation

$$(T + V_{n-e} + V_H)\psi_{n\mathbf{k}}(\mathbf{r}) + \int d\mathbf{r}' \, \Sigma \, (\mathbf{r}, \mathbf{r}', E_{n\mathbf{k}}^{QP})\psi_{n\mathbf{k}}$$
$$= E_{n\mathbf{k}}^{QP} \psi_{n\mathbf{k}}, \tag{1}$$

where T is the kinetic energy, V_H is the Hartree potential, and V_{n-e} is the potential due to the nuclear interaction with the electrons. $\Sigma(\mathbf{r}, \mathbf{r}', E_{n\mathbf{k}}^{QP})$ is the self-energy operator defined by

$$\Sigma(\mathbf{r}, \mathbf{r}', E_{n\mathbf{k}}^{QP}) = \frac{i}{4\pi} \int_{-\infty}^{\infty} e^{iE'\delta} G(\mathbf{r}, \mathbf{r}', E_{n\mathbf{k}}^{QP} + E')$$
$$\times W(\mathbf{r}, \mathbf{r}', E')dE'. \tag{2}$$

The screened Coulomb potential $W(\mathbf{r}, \mathbf{r}', E)$ was calculated from the polarizability matrix in the random-phase approximation, δ is a positive infinitesimal, and G is Green's function of the system.

This approximation is used with the LDA wavefunctions, correcting the typical LDA gap error in metal oxides, yielding normally very good band-gap energies.[11–14] Moreover, the present partially self-consistent GW$_0$ method also

corrects the LDA problem to localize the Zn 3 d-state which affects the Zn$_d$–O$_p$ hybridization at about 7 eV below the valence band maximum.[21] From the quasi-particle energy, Eq. (1), the difference between the energetically lowest unoccupied and highest occupied states gave a direct band-gap energy of E$_g$(GW$_0$) = 3.33 eV for ZnO, in very good agreements with the measured value.

The absorption coefficient was obtained from linear optical response, where first the imaginary part of the dielectric function, $\varepsilon(E) = \varepsilon_1(E) + i\varepsilon_2(E)$, was determined. This was obtained in the long wavelength limit, $\varepsilon_2(E) = \mathrm{Im}[\varepsilon(\mathbf{q} \to 0, E)]$, directly from the electronic structure, calculating the interactions between the pseudo-wavefunctions of the valence band ($u_{v\mathbf{k}}$) and the conduction band ($u_{c\mathbf{k}}$) through[22]

$$\varepsilon_2^{\alpha\beta}(E) = \frac{8\pi^2 e^2}{\Omega} \lim_{q \to 0} \frac{1}{q^2} \sum_{c,v,\mathbf{k}} w_{\mathbf{k}} \cdot \delta(E_{c\mathbf{k}}^{QP} - E_{v\mathbf{k}}^{QP} - E)$$
$$\times \langle u_{c\mathbf{k}+e_\alpha q}|u_{v\mathbf{k}}\rangle \langle u_{c\mathbf{k}+e_\beta q}|u_{v\mathbf{k}}\rangle^*, \tag{3}$$

where Ω is the volume of the primitive cell, $E_{c\mathbf{k}}^{QP}$ and $E_{v\mathbf{k}}^{QP}$ are the energy of states of the conduction and the valence band, respectively, e_α and e_β are unit vectors in the Cartesian directions, and $w_{\mathbf{k}}$ is the weight of the k-points to allow k-space summation over the irreducible part of the Brillouin zone.

The real part of the dielectric function, $\varepsilon_1(E)$, was obtained from $\varepsilon_2(E)$ by using the Kramers-Kronig transformation relation.[12] The absorption coefficient $\alpha(E)$ was thereafter obtained from $\varepsilon_1^2(E) + \varepsilon_2^2(E) = [\varepsilon_1(E) + \alpha^2(E)c^2/2E^2]^2$, where c is the speed of light. In order to compare the zero-temperature calculations with the room-temperature PAS measurements, we included an energy shift by -0.15 eV of the calculated band gap as well a 50 meV Lorentzian broadening in the calculated absorption spectrum.

III. RESULTS

To verify the influence of substrates on the optical properties of ZnO films, we carried out experiments on films deposited on *n*- and *p*-type non-porous silicon (flat Si) and
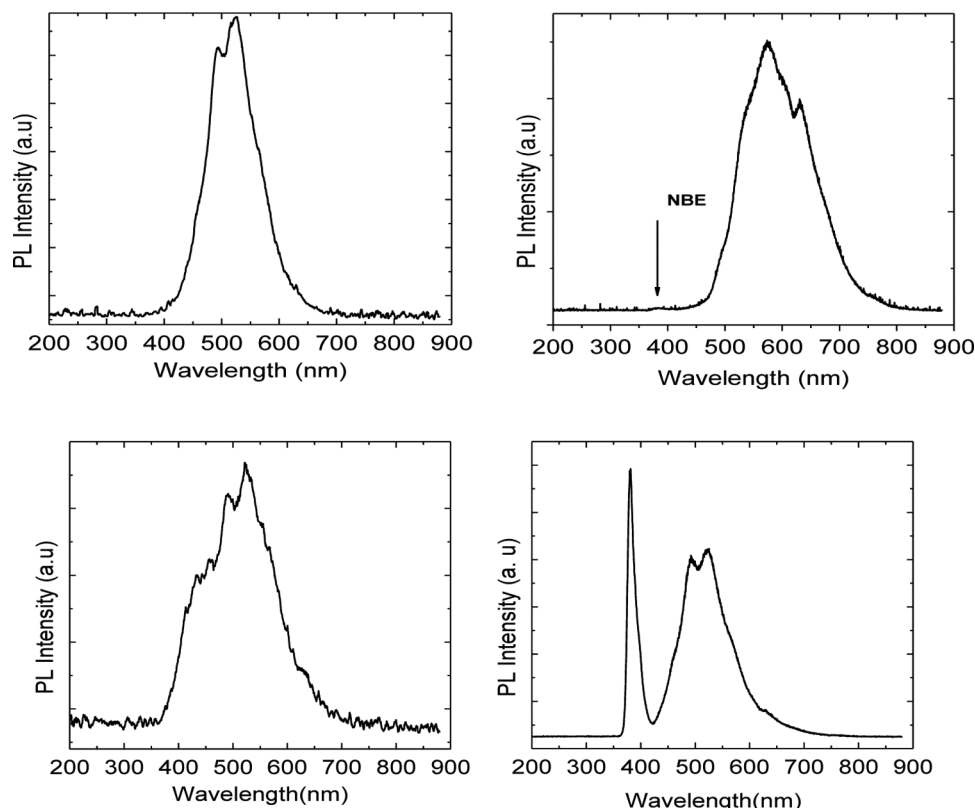
FIG. 4. (a) RT PL spectrum of ZnO film grown on n-Si (left) and ZnO film grown on p-PSi (right), the small peak at 383 nm is assigned to the ZnO NBE emission and (b) RT PL spectrum of ZnO film grown on p-Si (left) and ZnO film (right).

porous silicon (PSi) substrates. Luminescence imaging was acquired to provide a fast evaluation of the morphology and homogeneity of the samples. Fig. 3 depicts the single color luminescence images of a ZnO film deposited on a p-Si wafer. The integration times were 20 s, 15 s, and 300 s for the red, green, and blue colors, respectively.

Figure 4(a) presents the PL spectra of ZnO film deposited on n-Si and p-PSi. Fig. 4(b) shows the PL spectra of ZnO film on p-Si and only ZnO film. It is characterized by a dominant and broad emission band extending between 450 and 800 nm, with peak around 575 nm. In addition, a weak peak is observed around 383 nm, which is close to 379 nm, the near band edge (NBE) emission peak observed in high-quality bulk ZnO sample, measured under identical condition. The 575 nm broad emission band peaks at longer wavelength than that of the bulk ZnO at ~510 nm. The latter has been assigned to recombination process involving electrons trapped at a single oxygen vacancy with photo-generated holes.[17] Additional experiments must be performed to obtain insights about that nature of the broad band, which may have more than one component, as indicated by Borseth *et al.*[23] The observation of the NBE emission is consistent with the deposition of good quality ZnO films. The small strength of the peak may result from the low power excitation condition, which favor the long time recombination processes associated with the broad emission band. Measurements with different excitation conditions and temperature will be carried out to verify the nature of the dominant recombination processes.

Bulk ZnO wafer was measured to obtain reliable references, which yielded an energy gap around $E_g = 3.09$ eV. The samples of silicon p-type (p-Si, Eg = 3.17; p-Psi,

Eg = 3.15) and n-type Si (n-Si, Eg = 3.13; n-PSi) show a broad band of absorption between 350 nm and 450 nm, as depicted in Figure 5. Optical transition around 3.2 eV was observed in most of the ZnO films deposited on those substrates; however, it was not possible to observe the optical transition assigned to the ZnO film deposited on the n-PSi substrate, because its small thickness, i.e., less than 1 μm. Extremely high frequency modulation experiments are required to probe very thin films, as even for higher as 50 Hz the photoacoustic signal did not present satisfactory feature.

Figure 5 illustrates the photoacoustic absorption (PAS) spectra of the samples ZnO, n-Si + ZnO, n-PSi + ZnO, p-Si + ZnO, p-PSi + ZnO, and GW_0 results for ZnO film absorption. The errors associated with experimental measures were calculated from the expression of propagation of errors $\Delta E = |dE/d\lambda| \cdot \Delta\lambda = E \cdot \Delta\lambda/\lambda$, where $\Delta\lambda = 12$ nm is the
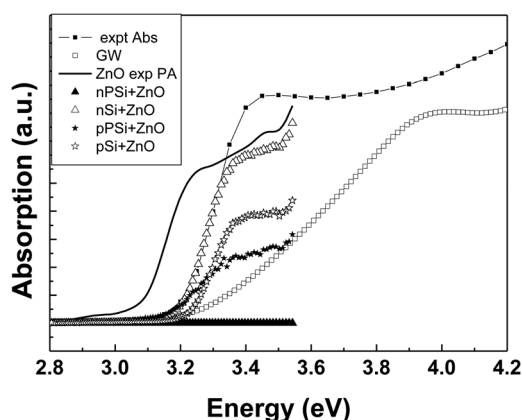

FIG. 5. Absorption results for ZnO based Si and PSi.

TABLE I. Comparison between PA experiment and the theory for the energy gap and by ellipsometry measurements on $ZnO_{1-x}S_x$ in a bulk wafer deposited by ALD.[24]

	Theory ZnO GW$_0$	Experiment ZnO	Experiment (Ref. 24)	Experiment n-Si + ZnO	Experiment p-Si + ZnO	Experiment p-Si + ZnO
Beginning absorption (eV)	3.33	3.09	3.31	3.13	3.17	3.15

resolution of the monochromator. The measured energy gaps of the different samples are shown in Table I, note that the discrepancy for the ZnO film is less than 10%. This discrepancy can be noticed as well between theory and experiment taken, respectively, at zero and room temperature band gap energies leading to a lower energy to the latter one.

To better understand the measured PAS absorption, we compared it with the corresponding calculated spectrum of bulk ZnO (Fig. 5). The present partially self-consistent GW$_0$ (GW$_0$) result yields very accurate zero-temperature band-gap energy: $E_g = 3.33$ eV. With the -0.15 eV shift, to account for temperature effect on the gap, the calculated onset to absorption agreed very well with the measured PAS results. The theoretical spectrum shows a continuous increase of the absorption for energies from 3.2 eV to ~ 4 eV, whereas the measured spectra show strong absorption in the range of 3.1–3.3 eV region. It is worthwhile to point out that our results are comparable to the finding by ellipsometry measurements on $ZnO_{1-x}S_x$ bulk wafer deposited by atomic layer deposition (ALD), revealing an energy gap of ~ 3.31 eV.[24] Moreover, in that work, both the strong exciton peak in ZnO (i.e., x = 0) at about 3.4 eV and the absorption peak at 4.2 eV can be verified by our measured and calculated absorption spectra, respectively. Since two-particle excitation effects are not included in the GW$_0$ method, the strong measured absorption in the range of 3.1–3.3 eV region is identified as absorption of electron-hole exciton pairs. We, therefore, suggest that excitons are present in these films, and one should thus be able to benefit from the excitonic effects also in devices with ZnO nanopillars.

IV. CONCLUSION

ZnO nanopillars were successfully grown using both the ACG and VLS methods on n- and p-type flat and porous Si. PL results indicate that good quality ZnO films were deposited on these substrates, with a weak NBE peak around 383 nm and a broad emission band between 450 and 800 nm. The optical absorption measured from all samples, using photoacoustic spectroscopy, was compared with a bulk ZnO wafer and the calculated absorption. The calculations were performed within the PAW/GW$_0$ approximation.

The theoretical result shows reasonable good agreement with experimental data for ZnO, despite that the GW$_0$ approach cannot describe excitonic effects, losing the sharp increase in the absorbance due to it. The values of the energy gaps of the ZnO films deposited on *n*-Si and *p*-Si, obtained by the photoacoustic technique, are shifted to the ultra-violet spectral region when compared with the theoretical and experimental data of bulk ZnO.

[1]S. M. Al-Hilli, R. T. Al-Mofarji, P. Klason, M. Willander, N. Gutman, and A. Sa'ar, J. App. Phys. **103**, 014302 (2008).
[2]G. Zheng, F. Patolsky, Y. Cui, W. U. Wang, and C. M. Lieber. Nat. Biotechnol. **23**, 1294 (2005).
[3]S. Al-Hilli, A. Öst, P. Stalfors, and M. Willander. J. Appl. Phys. **102**, 084304 (2007).
[4]M. Willander, K. ul Hassan, O. Nur, A. Zainelabdin, G. Amin, and S. Zaman, J. Mater. Chem. **22**, 2337 (2012).
[5]Q. X. Zhao, P. Klason, and M. Willander, Appl. Phys. A. **88**, 27 (2007).
[6]N. Gutman, A. Armon, A. Sa'ar, A. Osherov, and Y. Golan Appl. Phys. Lett. **93**, 073111 (2008).
[7]A. Ferreira da Silva, N. Veissid, C. Y. An, I. Pepe, N. Barros de Oliveira, and A. V. Batista da Silva, Appl. Phys. Lett. **69**, 1930 (1996).
[8]J. L. Gole, E. Veje, R. G. Egeberg, A. Ferreira da Silva, I. Pepe, and D. A. Dixon. J. Phys. Chem. B. **110**, 2064 (2006).
[9]G. Kresse and D. Joubert, Phys. Rev. B **59**, 1758 (1999).
[10]P. E. Blöchl, Phys. Rev. B **50**, 17953 (1994).
[11]M. Shishkin and G. Kresse, Phys. Rev. B **75**, 235102 (2007); F. Fuchs, J. Furthmüller, F. Bechstedt, M. Shishkin, and G. Kresse, *ibid*. **76**, 115109 (2007).
[12]A. Ferreira da Silva, I. Pepe, J. S. de Souza, C. Moyses Araujo, C. Persson, R. Ahuja, B. Johansson, C. Y. Yang, and J.-H. Guo, Phys. Scr. **T109**, 180 (2004).
[13]C. Persson and A. Ferreira da Silva, Appl. Phys. Lett. **86**, 231912 (2005).
[14]M. Shishkin, M. Marsman, and G. Kresse, Phys. Rev. Lett. **99**, 246403 (2007).
[15]V. Lehman and H. Föll, J. Electrochem. Soc. **137**, 653 (1990).
[16]V. Lehmann and U. Grüning, Thin Solid Films **297**, 131 (1997).
[17]L. Vayssieres, K. Keis, S. E. Lindquist, and A. Hagfeldt, J. Phys. Chem. B **105**, 3350 (2001).
[18]M. A. Mastro, J. A. Freitas, Jr., R. T. Holm, C. R. Eddy, Jr., J. Caldwell, K. Liu, O. Glembocki, R. L. Henry, and J. Kim. Appl. Surf. Sci. **253**, 6157 (2007).
[19]J. Ahn, M. A. Mastro, J. A. Freitas, Jr., H.-Y. Kim, R. T. Holm, C. R. Eddy, Jr., J.Hite, S. I. Maximenko, and J. Kim, Thin Solid Films **517**, 1111 (2008).
[20]A. Ferreira da Silva, M. V. Castro Meira, J. A. Freitas, Jr., G. Baldissera, C. Persson, N. Gutman, A. Sa'ar, P. Klason, and M. Willander, in *Tech. Proc. Nanotech.* (2009), Vol. 3, pp. 206–209.
[21]C. Persson, C. L. Dong, L. Vayssieres, A. Augustsson, T. Schmitt, M. Mattesini, R. Ahuja, J. Nordgren, C. L. Chang, A. Ferreira da Silva, and J.-H. Guo, Microelectron. J. **37**, 686 (2006).
[22]M. Gajdoš, K. Hummer, G. Kresse, J. Furthmüller, and F. Bechstedt, Phys. Rev. B, **73**, 045112 (2006).
[23]T. M. Borseth, B. G. Svensson, A. Yu. Kuznetsov, P. Klason, Q. X. Zhao, and M. Willander, Appl. Phys. Lett. **89**, 262112 (2006).
[24]C. Persson, C. Platzer-Björkman, J. Malmström, T. Törndahl, and M. Edoff, Phys. Rev. Lett. **97**, 146403 (2006).